GEOPHYSICAL RESEARCH LETTERS, VOL. 23, NO. 23, PAGES 3289-3292, NOVEMBER 15, 1996

Gravity-wave-scale temperature fluctuations seen by the UARS MLS

D. L. Wu and J. W. Waters

Jet Propulsion Laboratory, California Institute of Technology, Pasadena, California

Abstract - The Upper Atmosphere Research Satellite (UARS) Microwave Limb Sounder (MLS) has observed small- and meso-scale temperature fluctuations during a special limb-tracking operation. Analysis of late-December 1994 data shows that there exist significant radiance fluctuations with horizontal scales of 10's-100's km associated with upper tropospheric convection and the stratospheric polar vortex. Phase coherence and amplitude growth with height are observed, showing the presence of vertically propagating waves. Variance maps generated for the limb-tracking days further show that the MLS instrument can measure horizontal temperature variations at scales less than 100km in both limb-scanning and limb-tracking observation modes.

Introduction

Geographical and spectral distributions of gravity waves are crucial in determining their overall forcing on large-scale circulation and local mixing in the atmosphere. Measurement of these distributions has been provided by various techniques such as radar [Meek et al. 1985; Vincent and Fritts 1987; Fukao et al. 1994], lidar [Wilson et al. 1991], balloon [Allen and Vincent 1995], rocket [Hirota 1984], aircraft [Nastrom and Gage 1985] and satellite [Fetzer and Gille 1994]. Radar/lidar/balloon/rocket observations yield good temporal and vertical resolutions usually at one geographical station while aircraft observations provide a better geographical coverage for a short period of time. It is difficult in general for satellite techniques to obtain the same resolutions, but observations of atmospheric temperature variances at somewhat larger scales are possible, which are indicative of gravity wave activity, have recently been made by the Upper Atmosphere Research Satellite (UARS) Microwave Limb Sounder (MLS) using saturated 63GHz radiance profiles [Wu and Waters 1996].

In this letter we present the results from a non-standard MLS limb-tracking operation mode, which can provide more useful information for studying small-scale variability in the atmosphere than the normal limb-scanning mode. This MLS observation mode, in which the instrument field-of-view continuously tracks the atmospheric limb at ~18km tangent height, has been implemented periodically since December 1994 and should be able to provide a better gravity-wave climatology than the normal operation mode. The objectives of this letter are to describe the instrument sensitivity and measurement characteristics of the limb-tracking operation mode for gravity-wave studies, and discuss and interpret some features observed from it.

Limb-Tracking Operation

The MLS, in operation since 12 September 1991, was designed to measure profiles of molecular abundances (O_3, ClO, and H_2O), temperature and pressure in the middle atmosphere using emission features near 63, 183 and 205 GHz [Waters 1993; Barath et al. 1993]. Two sampling schemes have been used to observe the atmosphere: limb-scanning and limb-tracking. In normal limb-scanning mode the instrument step-scans the atmospheric limb in ~65 seconds from 90km to the surface at increments of ~5km in the mesosphere and 1-3km in the stratosphere and troposphere. When the instrument views tangent heights below 18km, all the 63GHz radiances are saturated (i.e., have optical depths much greater than 1) and provide atmospheric temperature measurements at various altitude layers. Thus, fluctuations in the saturated radiances directly reflect atmospheric temperature variations, which can be used to map gravity wave activity [Wu and Waters 1996]. In limb-tracking mode the instrument usually tracks the limb at ~18km tangent height and performs its usual 2-second sampling frequency, which is equivalent to ~15km horizontal resolution along the suborbital track. Since all 63GHz channel radiances are optically-thick in the 18km-limb-tracking mode, the radiance brightness yields atmospheric temperature with a good horizontal resolution and long sequence of measurements. Such data are very useful for studying geographical and spectral distributions of gravity waves.

Figure 1 shows the suborbital tracks of MLS samples on 28 December 1994 with a high sampling rate along the track. As illustrated in the inset, individual measurement locations are separated by horizontal displacements of ~15km with a larger gap when the instrument takes 6 seconds for calibration. The limb-tracking mode was used nearly continuously during 23-30 Dec. 1994, 1 Feb.-20 Mar. and 7-15 Apr. 1995, and scheduled for every-third-day operation since then while MLS is on. (Because of degradation in the UARS power system, the instruments on board are now operated in a time-shared mode). We do not present measurements from channels 1-2 and 14-15 because these channels are not always fully saturated and pointing variations may contaminate their radiance variances.

Temperature Weighting Functions

The temperature weighting functions for the saturated radiances have been previously described in Wu and Waters

Paper number 96GL02924.
0094-8534/96/96GL-02924$05.00

Table 1. The MLS 63GHz radiometer channel noise and temperature weighting function parameters

Channel	Layer Altitude (km)	Layer Thickness (km)	Noise (K)
1 and 15	~28	~10	~0.07
2 and 14	~33	~10	~0.08
3 and 13	~38	~10	~0.12
4 and 12	~43	~10	~0.18
5 and 11	~48	~10	~0.26
6 and 10	~53	~10	~0.37
7 and 9	~61	~10	~0.49
8	~80	~15	~0.45

(1996), showing that the altitude of saturation layers ranges from 28 to 80km for the different channels. As discussed therein, the fluctuations in the 63GHz saturated radiances are primarily due to instrument noise and atmospheric temperature fluctuation. Table 1 summarizes the MLS temperature weighting function parameters and noise for the 63GHz channels.

It is important to consider the 3-dimensional nature of the weighting functions since atmospheric waves can propagate vertically as well as horizontally and the observed amplitude of radiance fluctuations depends on the orientation of the weighting function relative to wave propagation direction. Figure 2(a) illustrates the asymmetry of the temperature weighting functions in the vertical plane, schematically showing slightly upward tilting from the horizontal plane. Because of the spatial asymmetry of the weighting functions, the observed magnitude of radiance fluctuations depends on the angle between line-of-sight and wave vector. For the same wave amplitude, the observed radiance fluctuations are larger if the line-of-sight is aligned more along with wavefronts. Asymmetry of the weighting functions appears also in the horizontal plane, as illustrated in Figure 2(b) with the measurement footprints. The width and length of these footprints are respectively ~20km and 150-300km. Similarly, this asymmetry can affect the observed magnitude of radiance fluctuations. Because of the UARS orbital geometry, the MLS is more sensitive to meridionally-propagating waves near the equator and more sensitive to zonally-propagating waves near the orbit turning latitudes (Figure 1).

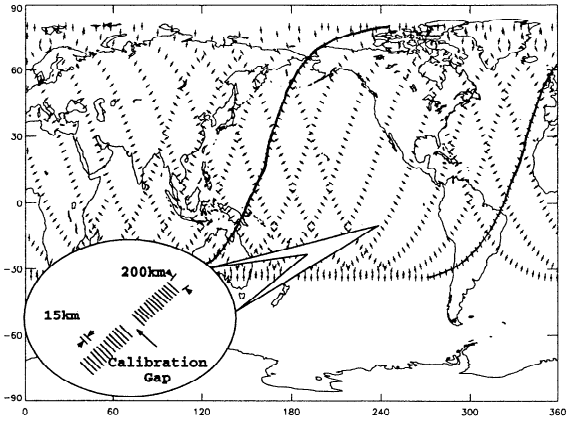

Figure 1. UARS/MLS sampling tracks on 28 December 1994 marked by the first measurement of each major frame (65.5 seconds). The inset details the set of individual measurements in a single major frame with the short lines indicating the orientation of the temperature weighting functions (see text). The UARS orbit is circular at 598km and the MLS viewing direction is 90° from the satellite velocity vector, which yields a latitudinal coverage from 34° of one hemisphere to 80° of the other. On this day MLS was preferentially observing the Northern Hemisphere. Orbits 1 (right) and 8 (middle) are highlighted with solid lines.

Radiances and Fluctuations

The radiance brightness temperature observed at 18km tangent height is a strong function of latitude due to atmospheric temperature climatology. As shown in Figure 3 for 28 December 1994, the brightness temperatures from channels 3-5 (at 38-48km altitudes) have large gradients near the vortex edge (~40-50°N) that dominate all other variations. The weak latitudinal gradients in channels 6-8 radiances suggest that the vortex is weakening at altitudes above 50km. The radiance gradient differs from orbit to orbit because the vortex in the Northern Hemisphere was not zonally symmetric at that time. Coherent variations can be seen in channels 7 and 8 at northern high-latitudes extending over thousands of kilometers due to strong wintertime planetary waves. Small-scale variations are also evident in many places. Caution

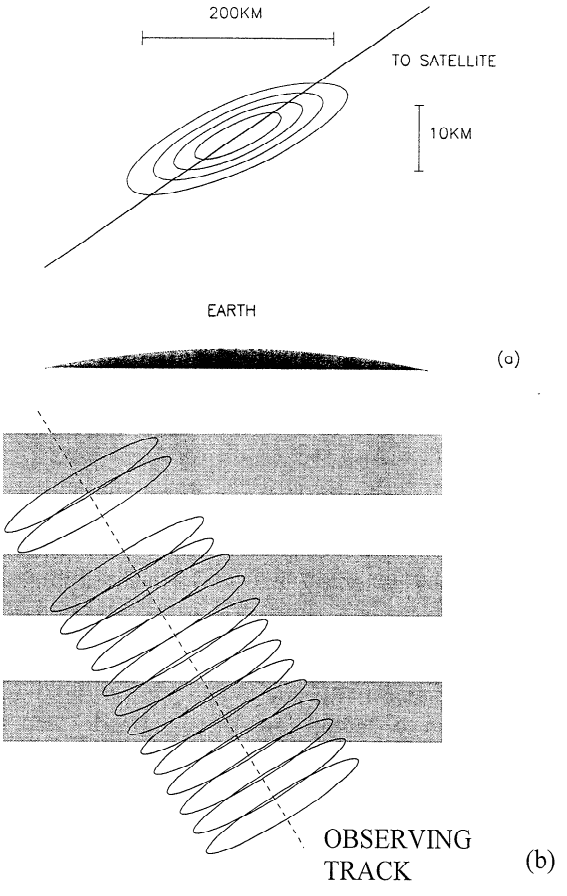

Figure 2. Temperature weighting functions for optically-thick 63GHz brightness at a low limb tangent height: a) in the vertical plane, and b) in the horizontal plane. The weighting function in a), normalized by its peak, is contoured at 0.2, 0.4, 0.6 and 0.8 from edge to center, while the line of sight is indicated by the straight line. The footprints in (b) illustrate the weighting functions relative to an assumed wave (shaded).

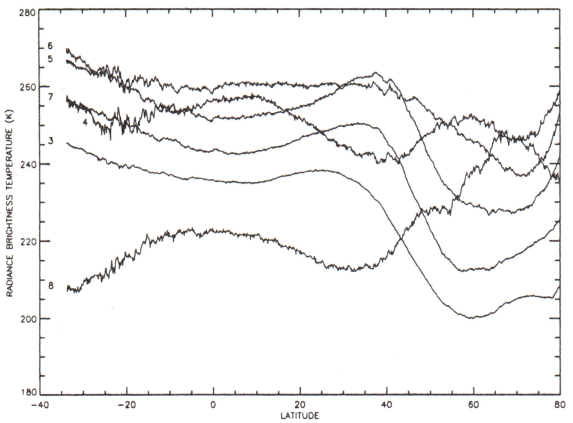

Figure 3. Channel 3-8 radiance measurements from the ascending part of orbit 1 on 28 December 1994. There are more samples near the orbit extremes at 34°S and 80°N than elsewhere. In the middle portion of the orbit, a 10° latitude bin corresponds to ~1300km in distance.

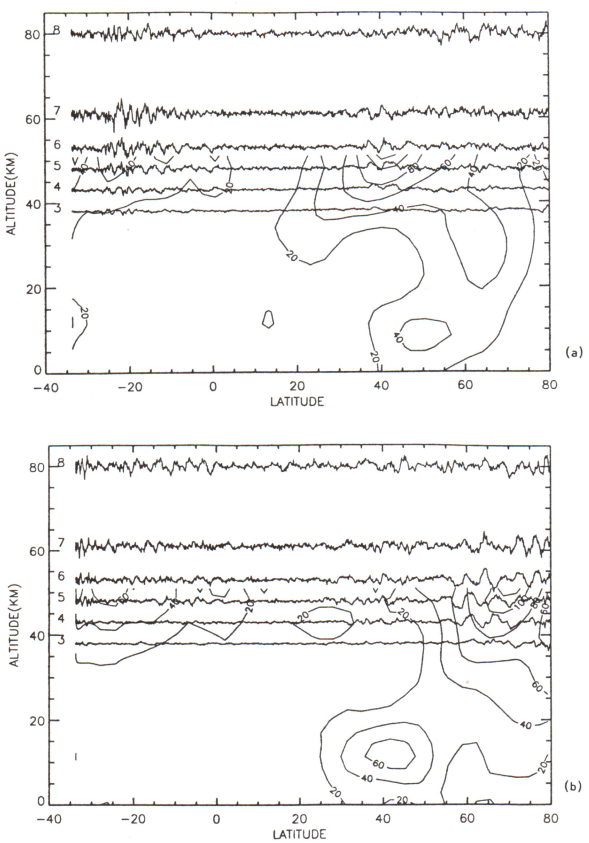

Figure 4. Observed radiance fluctuations as a function of latitude and altitude for orbits (a) 1 and (b) 8 after large-scale (>1000km) variations are removed. The wind speed along the observing track is contoured at intervals of 20ms^{-1}, which is obtained from a National Meteorological Center analysis and available only up to ~50km. The radiance fluctuations for each channel are displaced at its altitude levels with the same scale as height but a different unit (K). The channel number is indicated at the left of each measurement series. As seen in these examples, the strong background wind plays a key role in supporting wave growth and propagation.

should be given to the interpretation of large-scale radiance variations from channels 7-8. These channels and channel 9 (not shown in Figure 3), which are near the O_2 line center, may be affected (3-8K) by variations in the Zeeman effect due to Earth's magnetic field. Generally speaking, these changes vary slowly along the orbital track except above 70°N and below 25°S, for example during this observing day, where the viewing angle varies rapidly with respect to the magnetic field lines.

The small-scale fluctuations can be seen more readily in Figure 4 where large-scale (>1000km) variations are removed from the radiances in Figure 3. The data for Figure 4 are filtered by differencing the raw and smoothed data (averaged over ~1000km). Two orbits of data, separated by ~180° in longitude, are presented to show somewhat different features at middle and high latitudes. The data from the first ascending orbit [Figure 4(a)] display (0.5-3K) fluctuations at 10°-30°S over South America where strong deep convection is expected during this period. Oscillations with an amplitude of 1-2K are apparent at mid- and high-latitudes of the Northern Hemisphere, but are not as strong as in the Southern Hemisphere. This is likely due to the unfavorable viewing angle from the ascending orbit observing these propagating waves. As shown later in the variance maps, the observed radiance fluctuations are actually strong at these latitudes if one combines both ascending and descending measurements with different viewing angles. The important role of background wind speed is also evident in these observations, as has been emphasized in the recent numerical simulations

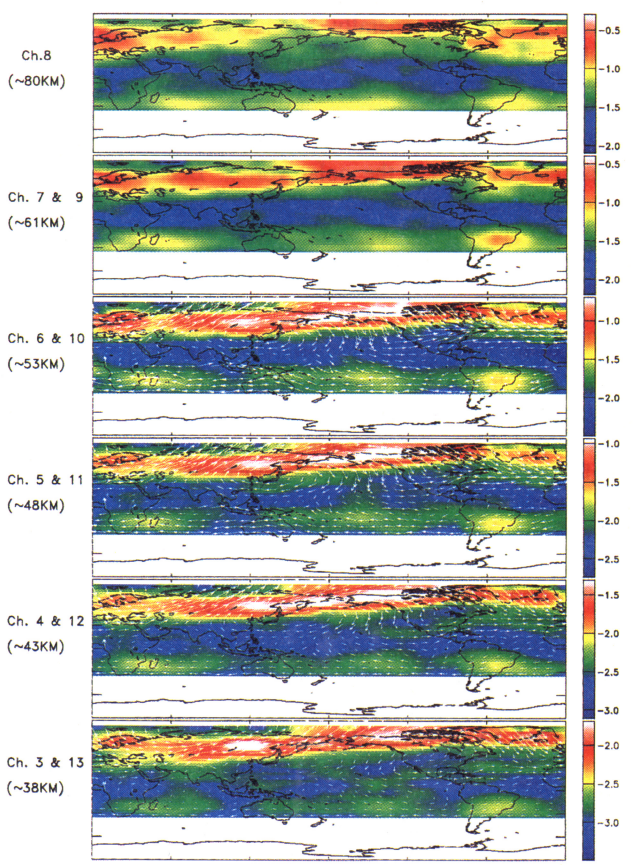

Figure 5. Radiance variance maps averaged for 23-30 December 1994. The variances, in units of K^2, are colored in a logarithmic scale, i.e., $\log_{10}(\sigma^2)$.

[Alexander 1996]. Phase coherence and amplitude growth with height are seen in regions of strong wind condition, reflecting the nature of vertically propagating waves. The data from orbit 8 (Figure 4b) show the presence of ~3K waves at high latitudes in the Northern Hemisphere which have scales of hundreds of kilometers. The 0-30°N region is relatively quiet for both orbits where measurements have very small fluctuations due mainly to instrument noise. It should be noted that the MLS radiance fluctuations may largely underestimate atmospheric temperature variations because of the broad vertical weighting functions. The observed magnitude of the radiance variance is expected to be determined by the gravity wave spectra, the MLS temperature weighting functions, and angles between the weighting function and wave vector. More accurate estimates for the scales and directions of waves to which MLS is sensitive require further study of MLS radiances for a model atmosphere with simulated gravity-waves.

Maps in Figure 5 are small-scale (<100km) radiance variances for 23-30 December 1994 limb-tracking days, produced by the technique described in Wu and Waters [1996]. Since measurements from a limb-tracking day produce four times as much data for this type of analysis as from a limb-scan day, the signal-to-noise ratio in these maps is about the same as that in the monthly mean obtained from scanning days. For the period analyzed here, the radiance variance shows similar enhancements along the polar jet in the Northern Hemisphere and over the strong tropospheric convection zones in the Southern Hemisphere as in Figure 3 of Wu and Waters [1996]. The variance associated with the polar jetstream is generally stronger over north Canada, Alaska and central Russia, while the variance associated with convectively generated gravity waves emerges most strongly over Brazil. Upward propagating gravity waves and vortex fine-structure are believed to cause the enhanced radiance variances in and near the polar vortex. Because the strong stratospheric jet provides a favorable condition for gravity waves to propagate upward, their amplitudes can be significantly amplified over one or two scale heights.

Summary

High-resolution MLS radiance measurements have been presented here to give overall characteristics of the radiance fluctuations when the instrument tracks the 18km tangent height. Gravity-wave-induced radiance perturbations stand out as a clear atmospheric signal. These wave-like variations grow with height in amplitude and are coherent in phase among the measurements at different altitude layers. This, and the analyses of Alexander [1996], have generally confirmed the interpretation of the observed variances by Wu and Waters [1996] as being due to gravity wave activity. The examples presented have demonstrated the horizontal resolution and long sequence of the new data set, which is expected to be very valuable for wave and vortex filament study. Because of spatial asymmetry of the instrument weighting functions, separate analyses of ascending and descending portions of the orbit can be used to infer vertical structures of the small-scale variability. Further study of this data set will be focused on the gravity wave spectrum and the structures of the strong radiance perturbations in the stratospheric polar vortex.

The radiance fluctuations induced by atmospheric gravity waves have been considered as "noise" to the MLS retrieval, in fact, to most remote sensing techniques. This "noise" is reflected in the Chi-square analysis or error budget analysis of desired products [e.g. Fishbein et al. 1996; Fetzer and Gille 1994]. However, the accurate and frequent MLS calibration allows the atmospheric portion to be extracted from the total radiance variance, providing observations of small-scale variability in the atmosphere.

Acknowledgments. We thank Bill Read, Evan Fishbein, Gloria Manney and Lee Elson for valuable discussions, and Robert Jarnot, Dennis Flower and Richard Lay for implementing the MLS limb-tracking mode. This work was performed at the Jet Propulsion Laboratory, California Institute of Technology, under contract with the National Aeronautics and Space Administration.

References

Alexander, M. J., A model of non-stationary gravity waves in the stratosphere and comparison to observations. in *Gravity Wave Processes and Their Parameterization in Global Climate Models* (K. Hamilton, ed.), New York: Springler-Verlag NATO ASI series, Vol. I, in press, 1996.

Allen, S.J., and R.A. Vincent, Gravity wave activity in the lower atmosphere: seasonal and latitudinal variations. *J. Geophys. Res.*, **100**, 1327-1350, 1995.

Barath, F.T., et al., The Upper Atmosphere Research Satellite Microwave Limb Sounder instrument, *J. Geophys. Res.* **98**, 10,751-10,762, 1993.

Fetzer, E.J., and J.C. Gille, Gravity wave variance in LIMS temperatures. Part I: Variability and comparison with background winds. *J. Atmos. Sci.*, **51**, 2461-2483, 1994.

Fishbein, E. F., R.E. Cofield, L. Froidevaux, R.F. Jarnot, T. Lungu, W.G. Read, Z. Shippony, J.W. Waters, I.S. McDermid, Validation of UARS MLS temperature and pressure measurements, *J. Geophys. Res.*,**101**, 9983-10,10016, 1996.

Fukao, S., M.D. Yamanaka, N. Ao, W.K. Hocking, T. Sato, M. Yamamoto, T. Nakamura, T. Tsuda, and S. Kato, Seasonal variability of vertical eddy diffusivity in the middle atmosphere, 1. three-year observations by the middle and upper atmosphere radar. *J. Geophys. Res.*, **99**, 18,973-18,987, 1994.

Hirota, I., Climatology of gravity waves in the middle atmosphere. *J. Atmos. Terr. Phys.*, **46**, 767-773, 1984.

Hirota, I., and T. Niki, A statistical study of inertia-gravity waves in the middle atmosphere. *J. Meteor. Soc. Japan*, **63**, 1055-1066, 1985.

Meek, C. E., I. M. Reid, and A. H. Mason, Observations of mesospheric wind velocities 2. Cross sections of power spectral density for 48-8 hours, 8-1 hours, and 1 hour to 10 min over 60-110km for 1981. *Radio Sci.*, **20**, 1383-1402, 1985.

Nastrom, G.D., and K.S. Gage, A climatology of atmospheric wave number spectra observed by commercial aircraft, *J. Atmos. Sci.*, **42**, 950-960, 1985.

Vincent, R.A., and D.C. Fritts, A climatology of gravity wave motions in the mesopause region at Adelaide, Australia. *J. Atmos. Sci.*, **44**, 748-760, 1987.

Waters, J. W., Chap.8 in *Atmospheric Remote Sensing Microwave Radiometry*, M.A. Janssen, Ed., Wiley, New York, pp.383-496, 1993.

Wilson, R., M.L. Chanin, and A. Hauchecorne, Gravity waves in the middle atmosphere observed by Rayleigh Lidar: 2. Climatology. *J. Geophys. Res.*, **96**, 5169-5183, 1991.

Wu, D. L. and J. W. Waters, Satellite observations of atmospheric variances: a possible indication of gravity waves, *J. Res. Lett.*, in press, 1996.

D. L. Wu and J. W. Waters, Mail Stop 183-701, Jet Propulsion Laboratory, California Institute of Technology, 4800 Oak Grove Drive, Pasadena, CA 91109. (e-mail: dwu@camel.jpl.nasa.gov)

(Received: April 29, 1996; accepted July 31, 1996.)